

FAST-TIMING MEASUREMENTS IN  $^{100}\text{Zr}$  USING  
 $\text{LaBr}_3(\text{Ce})$  DETECTORS COUPLED WITH  
 GAMMASPHERE\*

E.R. GAMBA<sup>a,†</sup>, A.M. BRUCE<sup>a</sup>, M. RUDIGIER<sup>b</sup>, S. LALKOVSKI<sup>b,c</sup>  
 S. BOTTONI<sup>d</sup>, M.P. CARPENTER<sup>d</sup>, S. ZHU<sup>d</sup>, A.D. AYANGEAKAA<sup>d</sup>  
 J.T. ANDERSON<sup>d</sup>, T.A. BERRY<sup>b</sup>, I. BURROWS<sup>e</sup>, R.J. CARROL<sup>b</sup>  
 P. COPP<sup>f</sup>, M. CARMONA GALLARDO<sup>g</sup>, D.M. CULLEN<sup>h</sup>, T. DANIEL<sup>b</sup>  
 G. FERNÁNDEZ MARTÍNEZ<sup>i</sup>, J.P. GREENE<sup>d</sup>, L.A. GURGI<sup>b</sup>  
 D.J. HARTLEY<sup>j</sup>, R. ILIEVA<sup>b</sup>, S. ILIEVA<sup>i</sup>, R.V.F. JANSSENS<sup>d</sup>  
 F.G. KONDEV<sup>k</sup>, T. KRÖLL<sup>l</sup>, G.J. LANE<sup>l</sup>, T. LAURITSEN<sup>d</sup>, I. LAZARUS<sup>e</sup>  
 G. LOTAY<sup>b</sup>, C.R. NIȚĂ<sup>m</sup>, ZS. PODOLYÁK<sup>b</sup>, V. PUCKNELL<sup>e</sup>, M. REED<sup>l</sup>  
 P.H. REGAN<sup>b,n</sup>, J. ROHRER<sup>d</sup>, J. SETHI<sup>d</sup>, D. SEWERYNIAK<sup>d</sup>  
 C.M. SHAND<sup>b</sup>, J. SIMPSON<sup>e</sup>, M. SMOLEŇ<sup>o</sup>, V. VEDIA<sup>g</sup>  
 E.A. STEFANOVA<sup>p</sup>, O. YORDANOV<sup>p</sup>

<sup>a</sup>University of Brighton, Brighton, UK

<sup>b</sup>University of Surrey, Guildford, UK

<sup>c</sup>University of Sofia “St. Kl. Ohridski”, Bulgaria

<sup>d</sup>Physics Division, Argonne National Laboratory, Argonne, USA

<sup>e</sup>STFC Daresbury Laboratory, Daresbury, UK

<sup>f</sup>University of Massachusetts Lowell, Lowell, Massachusetts, USA

<sup>g</sup>Universidad Complutense, Madrid, Spain

<sup>h</sup>University of Manchester, Manchester, UK

<sup>i</sup>Technische Universität Darmstadt, Darmstadt, Germany

<sup>j</sup>Department of Physics, U.S. Naval Academy, Annapolis, USA

<sup>k</sup>Nuclear Engineering Division, Argonne National Laboratory, Argonne, USA

<sup>l</sup>Australian National University, Canberra, Australia

<sup>m</sup>Horia Hulubei National Institute of Physics and Nuclear Engineering  
 Bucharest-Măgurele, Romania

<sup>n</sup>AIR Division, NPL, Teddington, UK

<sup>o</sup>University of the West of Scotland, Paisley, UK

<sup>p</sup>Institute for Nuclear Research and Nuclear Energy, Sofia, Bulgaria

*(Received December 13, 2017)*

In order to investigate the evolution of nuclear deformation in the region of the chart of nuclides around mass numbers  $A \simeq 110$  and  $A \simeq 150$ ,

---

\* Presented at the XXXV Mazurian Lakes Conference on Physics, Piaski, Poland, September 3–9, 2017.

† Corresponding author: [E.Gamba@brighton.ac.uk](mailto:E.Gamba@brighton.ac.uk)

an experiment was performed at the Argonne National Laboratory where the gamma-decay radiation emitted from the fission fragments of  $^{252}\text{Cf}$  was measured using 51 Gammasphere detectors coupled with 25  $\text{LaBr}_3(\text{Ce})$  detectors. In this work, a short description of the experimental setup is presented together with some preliminary results from the fast-timing analysis of the  $4^+$  state of the nucleus  $^{100}\text{Zr}$ . A lifetime value of  $\tau = 50(28)$  ps was obtained using the Generalized Centroid Shift Method. This result agrees with the literature value of  $\tau = 53(4)$  ps within one standard deviation.

DOI:10.5506/APhysPolB.49.555

## 1. Introduction

Important information about the evolution of the deformation across the nuclear chart can be obtained from lifetime measurements of low-lying excited states in nuclei. The lifetime of the first excited states is an essential ingredient in the calculation of the reduced transition probability  $B(E2)$  which gives, in turn, the quadrupole moment related to the deformation parameter  $\beta_2$ . In this experiment, a source of  $^{252}\text{Cf}$  was used in order to populate the regions around mass numbers  $A \simeq 110$  and  $A \simeq 150$ . This source allowed to produce fission fragments with the highest yields in these deformed regions with respect to other fission sources [1]. Gamma rays emitted from the fission fragments were detected using a hybrid detector array made of 51 HPGe detectors from Gammasphere and 25  $\text{LaBr}_3(\text{Ce})$  scintillator detectors. These scintillator detectors were used in the past to measure lifetimes in the sub-nanosecond range [2, 3] and they have been used in many successful experiments, for example during the EXILL-FATIMA campaign [3] and at RIKEN [4]. The 25 scintillator detectors are part of the UK NuSTAR Collaboration [5, 6] and in this experiment they were coupled for the first time to a fully digital acquisition system.

## 2. The setup

The two hemispheres of the hybrid array were arranged in a  $4\pi$  geometry around the  $^{252}\text{Cf}$  fission source which was sandwiched between two platinum disks. The  $\text{LaBr}_3(\text{Ce})$  detectors consisted of a  $1.5'' \times 2''$  cylindrical crystal coupled with a R9779 Hamamatsu PMT. In order to reduce the Compton background and also the number of cross-talk events between neighbouring detectors, each detector was equipped with a lead shield. During the experiment, a typical  $\text{LaBr}_3(\text{Ce})$  count rate for one single detector was 2.7 kHz. Each array had its own acquisition chain which worked independently. A detailed description of the two acquisition systems can be found in Refs. [7, 8] for the digital Gammasphere acquisition (DGS), and in Ref. [9] for the  $\text{LaBr}_3(\text{Ce})$  coupled with DGS. The stand-alone DGS collected

3-fold events within a coincidence window of  $2\ \mu\text{s}$  for spectroscopic purposes. A second data set contained the fast-timing information which consisted of 2-fold events in the  $\text{LaBr}_3(\text{Ce})$  array, in coincidence with at least one gamma ray detected in Gammasphere. The time coincidence window between Gammasphere and the  $\text{LaBr}_3(\text{Ce})$  array events was set to 500 ns and the window between any two coincident events in the  $\text{LaBr}_3(\text{Ce})$  detectors was 200 ns.

### 3. Preliminary results

A preliminary measurement of the lifetime of the  $4^+$  state in  $^{100}\text{Zr}$  is presented in this section. In order to isolate the  $4^+$  state at 564 keV, a total of 16 different pairs of energy gates has been applied to the data set. The gates have been selected by using the independent DGS dataset to check for clean combinations of gates on the yrast band in  $^{100}\text{Zr}$  (excluding the  $6^+ \rightarrow 4^+$  and  $4^+ \rightarrow 2^+$  transitions) and on the even- $A$  fission partners  $^{146,148,150}\text{Ce}$ . This procedure gave the spectrum shown in Fig. 1 (left) where transitions from  $^{100}\text{Zr}$  and its fission partners are labelled. In Fig. 1 (right), the DGS energy spectrum with no gates applied is shown for comparison.

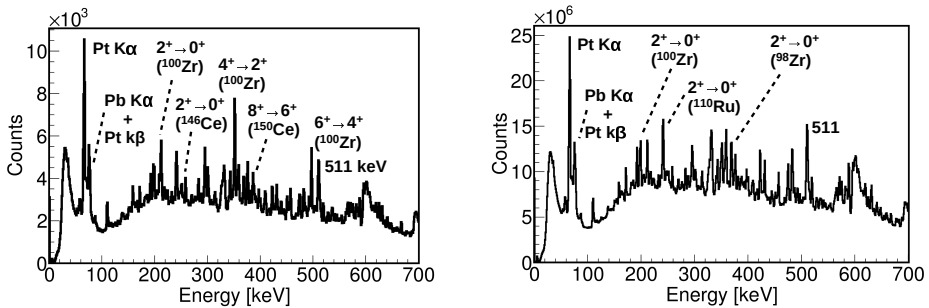


Fig. 1. Left: Sum of 16 double-gated DGS energy spectra. Right: Total DGS energy spectrum with no gates applied.

The  $\text{LaBr}_3(\text{Ce})$   $\gamma$ - $\gamma$  matrix shown in Fig. 2 (left) is produced by applying the same set of gates used for the DGS spectrum in Fig. 1 (left). The peak encircled in solid black/blue represents the coincidence between the  $6^+ \rightarrow 4^+$  and  $4^+ \rightarrow 2^+$  transitions, while the black dotted lines represent the graphical cuts used to estimate the contribution to the time distribution from the Compton background. In Fig. 2 (right), a DGS  $\gamma$ - $\gamma$  matrix shows the same energy regions as (left) after the gating procedure. The same graphical cuts are superimposed on this matrix to show that the background gates are relatively free from any contaminants. The histograms shown in Fig. 3 (left) represent the delayed and anti-delayed time distributions for the  $4^+$  state. The delayed curve (lighter/blue) has been obtained from the case where

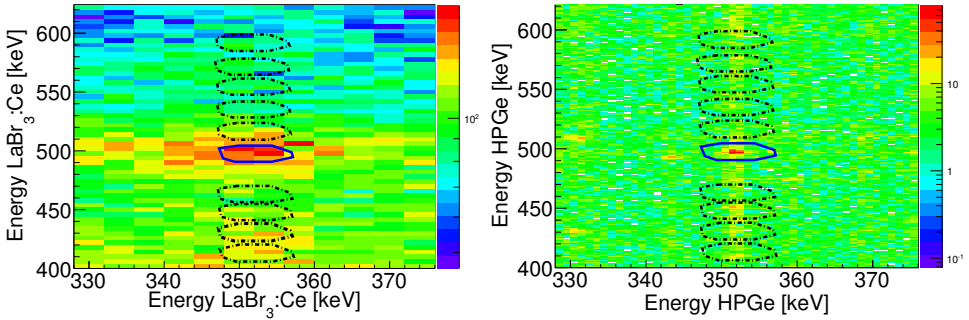


Fig. 2. (Colour on-line) Left:  $\gamma$ - $\gamma$  matrix for the  $\text{LaBr}_3(\text{Ce})$  array, obtained using the same gates as in Fig. 1 (left). With black/blue solid line is represented the cut on the coincidence peak for the cascade  $6^+ \rightarrow 4^+ \rightarrow 2^+$ , while the black dotted lines are the background cuts. Right: DGS  $\gamma$ - $\gamma$  matrix for comparison with (left).

the feeding transition  $6^+ \rightarrow 4^+$  is used as a start and the decay transition  $4^+ \rightarrow 2^+$  as the stop, while the anti-delayed distribution (darker/red) is obtained in the opposite case. The Generalized Centroid Difference method (GCD), described in Ref. [10], allows the determination of the lifetime of the state by measuring the centroid difference ( $\Delta C$ ) between these two time distributions. The  $\Delta C$  between these curves was measured as 184(16) ps, but has to be corrected for the value of the Prompt Response Distribution (PRD) curve and also for the time delay given by the background events underlying the full energy peak ( $\Delta C_{\text{Bg}}$ ). The PRD curve of this setup gives

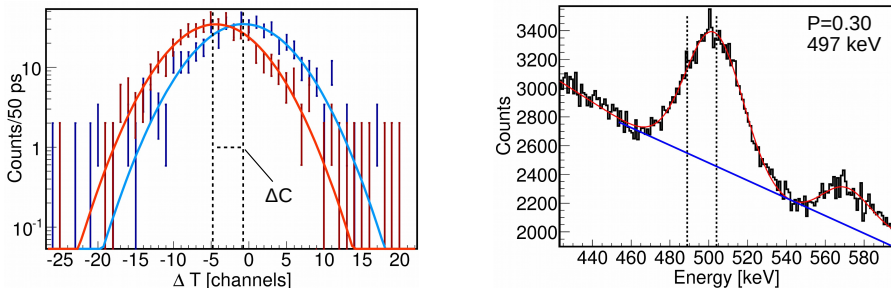


Fig. 3. (Colour on-line) Left: Centroid difference between the delayed (lighter/blue) and anti-delayed (darker/red) time distributions, obtained from the cascade  $6^+ \rightarrow 4^+ \rightarrow 2^+$  in  $^{100}\text{Zr}$ . Right: DGS-gated  $\text{LaBr}_3(\text{Ce})$  energy spectrum in the region around the 497-keV peak. The black dotted lines marks the cut limits used to obtain the time distributions. The descendant/blue line show the fitted linear background, and a peak-to-background ratio of 0.30 was determined for the channels inside the black dotted lines.

a value of 124(7) ps for the energy combination at 497 keV and 352 keV, and the background time correction is evaluated using the method described in Ref. [3]. The lifetime value is then calculated using the equation in Ref. [3]

$$\tau = \frac{1}{2} \left( \Delta C + \frac{\Delta C - \Delta C_{\text{Bg}}}{P} - \text{PRD} \right), \quad (1)$$

where  $P$  is the peak-to-background ratio of the energy transition at 497 keV. In Fig. 3 (left), the Gaussian fit for the peak at 497 keV ( $6^+ \rightarrow 4^+$ ), obtained from the  $\text{LaBr}_3(\text{Ce})$  array after applying the DGS gates, is shown (darker/red curve), together with the estimated linear background (lighter/blue line). The black dotted lines are the gate limits used to obtain the time distributions shown in Fig. 3 (right), taken to the left-hand side of the peak in order to minimize the contribution of the peak at 511 keV. A peak-to-background ratio of 0.30 has been measured for the region inside the dotted lines. In Fig. 4, the  $\Delta C$  values for the background contributions are shown by the lighter/blue dots. The background energies at which the points are plotted are the centroids of the graphical cuts in Fig. 2 (left) and these points were then fitted with the straight/red line shown in Fig. 4, using a  $\chi^2$  minimization algorithm.  $\Delta C_{\text{Bg}}$  is extracted from the background fit at the energy of 497 keV and its value is 174(14) ps. A similar analysis has been carried out for the peak at 352 keV and a  $\Delta C_{\text{Bg}}$  value of 168(20) ps was obtained, together with a  $P$  value of 0.28. The weighted average of the two lifetime values  $\tau = 65(47)$  ps and  $\tau = 45(36)$  ps, obtained by applying this procedure to both transitions, gives a lifetime value of  $\tau = 50(28)$  ps, consistent within one standard deviation with the literature value of  $\tau = 53(4)$  ps [3, 11, 12]. The large experimental error associated with this measurement

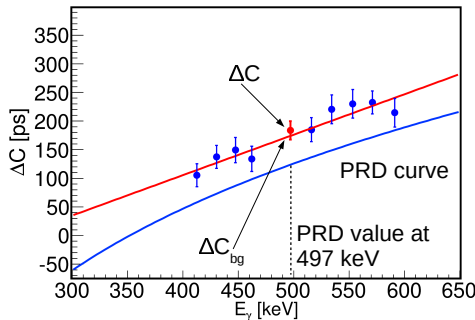


Fig. 4.  $\Delta C$  values for the background at different energies around the peak at 497 keV (lighter/blue dots). The straight/red line is the linear fit of these values, obtained via a weighted  $\chi^2$  minimization algorithm. The darker/red dot represents the  $\Delta C$  value for the  $6^+ \rightarrow 4^+ \rightarrow 2^+$  cascade.  $\Delta C_{\text{Bg}}$  was calculated to be 174 ps at the energy of 497 keV. The PRD curve is represented by the solid/blue line.

arises from the small  $P$  value which consequently enlarges the statistical errors (see Eq. (1)). An uncertainty of  $1\sigma$  was considered for both the PRD and the background curves.

#### 4. Conclusions

Together with the results presented in Ref. [9], this work shows that it is possible to measure level lifetimes as short as a few tens of picoseconds using the GCD method on this dataset. Both works show results consistent with the literature. The background selection procedure suggested in Ref. [3] has been successfully applied to these data for the first time.

UK authors acknowledge the support of the Science and Technology Facilities Council (STFC). E. Stefanova and O. Yordanov acknowledge support from BNSF under contract DFNI-E02/6.

#### REFERENCES

- [1] A.C. Wahl, Symposium on Physics and Chemistry of Fission, IAEA, 1965.
- [2] N. Mărginean *et al.*, *Eur. Phys. J. A* **46**, 329 (2010).
- [3] J.M. Régis *et al.*, *Nucl. Instrum. Methods Phys. Res. A* **763**, 210 (2014).
- [4] F. Browne *et al.*, *Phys. Lett. B* **750**, 448 (2015).
- [5] Zs. Podolyak, *Rad. Phys. Chem.* **95**, 14 (2014).
- [6] S. Lalkovski *et al.*, *Acta Phys. Pol. B* **47**, 637 (2016).
- [7] I-Y. Lee *et al.*, *Nucl. Phys. A* **520**, 641c (1990).
- [8] J.T. Anderson *et al.*, *IEEE NSS/MIC* **2012**, 1536 (2012).
- [9] M. Rudigier *et al.*, *Acta Phys. Pol. B* **48**, 351 (2017).
- [10] J.-M. Régis *et al.*, *Nucl. Instrum. Methods Phys. Res. A* **726**, 191 (2013).
- [11] H. Ohm *et al.*, *Z. Phys A* **334**, 519 (1989).
- [12] A.G. Smith *et al.*, *J. Phys G: Nucl. Part. Phys.* **28**, 2307 (2002).